Accepted Manuscript

Substituent effects on the isomerization of hydrazone switches driven by the intramolecular hydrogen bond

Chaocao Lu, Bu Htan, Shitao Fu, Chunmiao Ma, Quan Gan

PII: S0040-4020(19)30682-9

DOI: https://doi.org/10.1016/j.tet.2019.06.022

Reference: TET 30414

To appear in: *Tetrahedron*

Received Date: 9 May 2019

Revised Date: 11 June 2019

Accepted Date: 17 June 2019

Please cite this article as: Lu C, Htan B, Fu S, Ma C, Gan Q, Substituent effects on the isomerization of hydrazone switches driven by the intramolecular hydrogen bond, *Tetrahedron* (2019), doi: https://doi.org/10.1016/j.tet.2019.06.022.

Graphical Abstract

The substituents effects on the intramolecular hydrogen bonds of hydrazones further alter their isomerization.

Substituent effects on the isomerization of hydrazone switches driven by the intramolecular hydrogen bond

Leave this area blank for abstract info.

Chaocao Lu, Bu Htan, Shitao Fu, Chunmiao Ma, Quan Gan*

Hubei Key Laboratory of Bioinorganic Chemistry & Materia Medica, School of Chemistry and Chemical Engineering, Huazhong University of Science and Technology, Wuhan 430074, P. R. China.

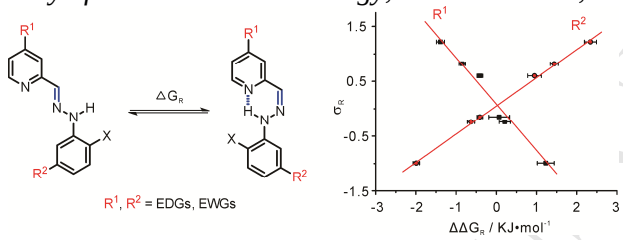

ELSEVIER

Tetrahedron

journal homepage: www.elsevier.com

Substituent effects on the isomerization of hydrazone switches driven by the intramolecular hydrogen bond

Chaocao Lu, Bu Htan, Shitao Fu, Chunmiao Ma, Quan Gan*

Hubei Key Laboratory of Bioinorganic Chemistry & Materia Medica, School of Chemistry and Chemical Engineering, Huazhong University of Science and Technology, Wuhan 430074, P. R. China.

ARTICLE INFO

Article history:
Received
Received in revised form
Accepted
Available online

Keywords:
Hydrazone switch
Hydrogen bond
Isomerization
Substituent effects

ABSTRACT

In this work, the substituent effects on hydrogen bonding in one kind of hydrazone-based switch are revealed. The E/Z isomerization ratios of these hydrazones and their intramolecular hydrogen bond strengths in the Z form were evaluated using NMR technique. Linear correlations between these parameters and Hammett empirical values for substituent effects are explored as well.

1. Introduction

Hydrogen bond is a topic of significant scientific study, as it plays an important role in the structure, function and dynamics of chemical and biological systems.[1–6] For example, the intermolecular hydrogen bonding is the main driving force for host-guest complexation in supramolecular chemistry.[7–11] The influence of the intramolecular hydrogen bond (IMHB) on the folding and unfolding of peptides and artificial analogs has been fully studied.[12–17] For some molecular switches, the IMHB has also been proved to take effect on the conversion of their configurations.[18,19] Recently, we and others have explored a series of acylhydrazones, where the E/Z isomerization was governed by the formation and breaking of IMHB.[20–22] To further explore the detail of the effects of the hydrogen bond on molecular switching, we herein report a series of hydrazone-based switches and investigate the relationship between the intramolecular hydrogen bonds and the isomerizations of the switches by systematically regulating the substituents.

In this study, the structures of the switches were optimized to a hydrazone framework wherein the IMHB is contained in a six-membered ring (HN−N=C−C=N) in the Z form (Scheme 1). As the N−H···N hydrogen bonding is the main driving force that governs the balance of E/Z isomerization in this system, the effect of IMHB can be accurately determined by the E/Z configurational equilibrium. This relation may further open up the possibility for the introduction of various substituents to evaluate the strength of IMHB that can be used to alter the molecular configuration. With this in mind, a series of hydrazone compounds **1**−**15** with different substituents were prepared (Scheme 1). The electronic properties of electron-donating groups (EDGs) and electron-withdrawing groups (EWGs) of the prepared compounds were quantified by the analysis of Hammett substituent constants.[23,24]

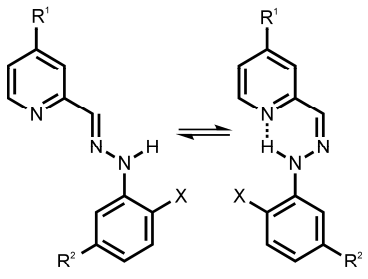

	X	R^1	R^2
1	F	H	H
2	Cl	H	H
3	Br	H	H
4	F	CN	H
5	F	CO_2Me	H
6	F	Cl	H
7	F	Me	H
8	F	OCH_3	H
9	F	$N(CH_3)_2$	H
10	F	H	CN
11	F	H	CO_2Me
12	F	H	Cl
13	F	H	Me
14	F	H	OCH_3
15	F	H	$N(CH_3)_2$

Scheme 1. The structures and isomerization equilibria of the hydrazone switches synthesized in this study.

* Corresponding author. e-mail: ganquan@hust.edu.cn (Q. Gan)

2. Results and discussion

2.1. ^{1}H NMR analysis of the hydrazones with different halogens

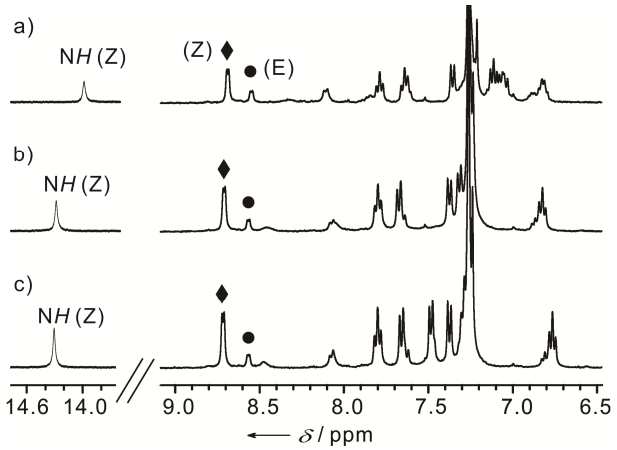

Fig. 1. Partial ^{1}H NMR spectra (400 MHz, $CDCl_3$, 298 K) for hydrazone **1**−**3** at equilibrium. Two signals for the aromatic protons from E/Z isomers were marked with filled circles and diamonds, respectively.

The E/Z isomers for all the compounds **1**−**15** can be separated by column chromatography due to the slow kinetics of isomerization, which has been reported for the related hydrazone derivatives.[21,25] The NMR technique was chosen for evaluating the hydrogen bonding, since it is well-known that the proton shifts are highly correlated with the hydrogen bond strength, i.e., the downfield shifts of the proton arisen from deshielding is increased with increasing hydrogen bond strength and vice versa.[26–28] To fast establish the relationship between the substituent effects and the intramolecular hydrogen bonds, the hydrazones **1**−**3** were firstly assessed as they are only varied with one substitution of halogen. For the Z isomers of hydrazones **1**−**3**, the downfield shift of the hydrazine N−H protons was observed from 13.98 to 14.31 ppm, which infers the hydrogen bond strength may increase when the substituent groups are varied from fluorine to chlorine and then to bromine (Fig. 1). On the other hand, the ratio of E/Z configuration at equilibrium can also be used as a standard for assessing the hydrogen bonding in our system. In general, along with the strength of IMHB gradually increased, the proportion of the Z isomers would increase correspondingly. The E/Z ratios for hydrazones **1**−**3** were calculated to be 0.41, 0.27 and 0.24, respectively, according to the integration of the aromatic signals by their NMR spectra at equilibrium (Fig. 1, Table 1). The results show the proportion of Z isomer for the hydrazone **1** is the lowest, while the hydrazone **3** has the highest proportion of the Z conformer. This order indicates that **3**−Z possesses the most stable IMHB compared to **1**−Z and **2**−Z. We attributed this difference to the anisotropy and the electronic effect of the halogen substitutions. The Van der Waals radius of Br is much larger than that of F, and the lone pairs are much more diffuse, thus the lone pairs of Br provide a larger anisotropic effect, which results in the enhancement of the adjacent IMHB.

2.2. Crystal structure analysis

Next, we examined the crystal structures of hydrazones **1**−**3** (Fig. S1−S6), because the hydrogen bond donor-acceptor atom distance can be used to evaluate the hydrogen bond strength.[29–32] The fine crystals for both E/Z isomers were obtained by slow diffusion of hexane to their corresponding chloroform solutions. The analysis of the crystal structures revealed that all structures adopt a nearly planar geometry and the hydrazine N−H protons are hydrogen-bonded with the pyridine nitrogens in the Z form.

Table 1. Summarizes of the N−H chemical shifts in Z isomer, ratio of E:Z and Gibbs free energy ΔG_R of E/Z equilibrium for componuds **1**−**15**.

	NH (ppm)	E:Z Ratio	ΔG_R (kJ/mol)
1	13.98	0.41 ± 0.02	2.20 ± 0.13
2	14.28	0.27 ± 0.02	3.24 ± 0.17
3	14.31	0.24 ± 0.02	3.54 ± 0.21
4	13.70	0.72 ± 0.03	0.81 ± 0.10
5	13.85	0.58 ± 0.02	1.35 ± 0.08
6	13.82	0.48 ± 0.02	1.79 ± 0.07
7	14.01	0.38 ± 0.02	2.41 ± 0.14
8	14.05	0.40 ± 0.04	2.27 ± 0.26
9	14.22	0.25 ± 0.02	3.43 ± 0.21
10	14.17	0.16 ± 0.01	4.54 ± 0.15
11	14.08	0.23 ± 0.01	3.64 ± 0.10
12	14.03	0.28 ± 0.02	3.15 ± 0.17
13	13.94	0.53 ± 0.02	1.57 ± 0.09
14	13.98	0.48 ± 0.02	1.79 ± 0.07
15	13.94	0.92 ± 0.03	0.21 ± 0.08

Further analysis of the crystal structures revealed that **3**−Z has the shorter N···H distance compared to that of **1**−Z (Fig. 2), apart from this, the N−H···N angle of **3**−Z is larger than that of **1**−Z, both of which mean the strength of IMHB in **3**−Z is stronger than that in **1**−Z. This result is consistent with NMR data that compound **3** possessing the highest Z form. Here, the six-membered ring (HN−N=C−C=N) hydrogen bond motif is similar to the classical resonance-assisted hydrogen bonding (RAHB) fragment (HO−CR=CR−CR=O).[33,34] The N···N distances and N−N bond lengths of N−H···N hydrogen bonds in our systems, by contrast, are longer than the reported bond distances of the same (HN−N=C−C=N) RAHB motif,[35] indicating the weaknesses of aromaticity in our RAHB fragment.

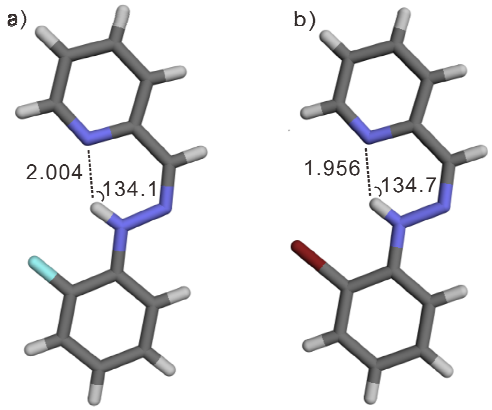

Fig. 2. Crystal structures of a) **1**−Z; b) **3**−Z. The dashed lines indicate hydrogen bonds.

2.3. ^{1}H NMR analysis of the hydrazones substituted on the pyridine ring

To further test the relationship between the substituent effects on the IMHB, the compounds **4**−**15** with different EDGs and EWGs substituents were examined. The analysis of ^{1}H NMR spectroscopy of the hydrazones **4**−**9** indicates the downfield shift of N−H resonance from 13.70 to 14.22 ppm with the variation in

substituent groups, suggesting a trend of the enhancement of the IMHB strength from EWG to EDG substitutions (Fig. 3, Table 1). The E/Z ratio variation also follows this trend. As the hydrogen bond strength becomes stronger, the proportion of Z isomers gradually increases. This regular change can be explained by two aspects. On one hand, the EWGs decrease the basicity of nitrogen in the pyridine ring, thus weakening the IMHB, while the EDGs direct the opposite effect. On the other hand, this result is also consistent with the RAHB mechanism, which reveals that the increase of electron-donating input can strengthen the hydrogen bonding through π-delocalization.[36–40]

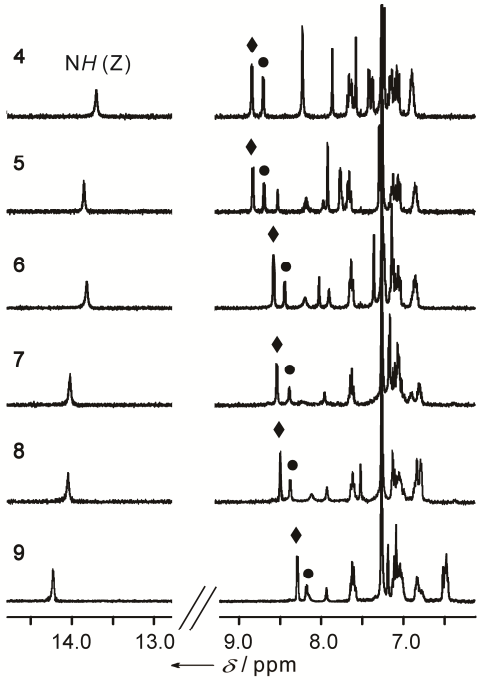

Fig. 3. Partial ^{1}H NMR spectra ($CDCl_3$, 400 MHz, 298 K) of **4**–**9** at equilibrium. Two signals for the aromatic protons from E/Z isomers were marked with filled circles and diamonds, respectively.

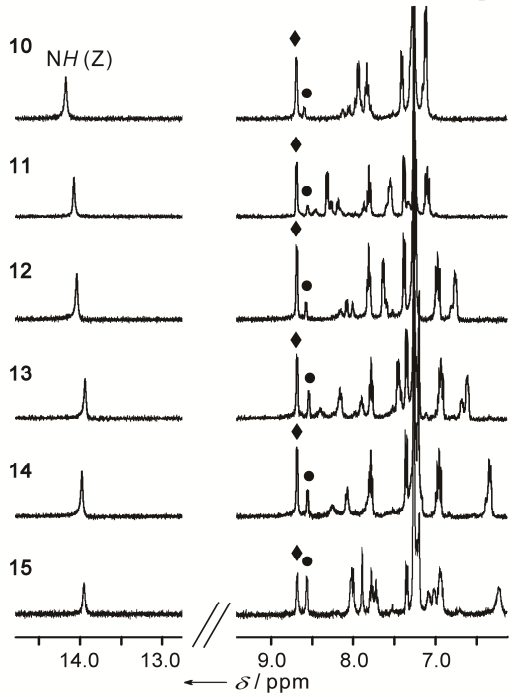

Fig. 4. Partial ^{1}H NMR spectra ($CDCl_3$, 400 MHz, 298 K) of **10**−**15** at equilibrium. Two signals for the aromatic protons from E/Z isomers were marked with filled circles and diamonds, respectively.

2.4. ^{1}H NMR analysis of the hydrazones substituted on the phenyl ring

The ^{1}H NMR spectral analysis of the hydrazones **10**−**15** shows a reverse trend of the substituent effects on the IMHB, i.e., the N−H resonances upfield shift by the replacement of EWGs to EDGs on the benzene rings. For instance, by changing the substitution from the CN to $N(Me)_2$ group, a shift in the N−H proton signals from 14.17 to 13.94 ppm can be observed (Fig. 4, Table 1). This was reasoned as the more EDGs it employs, the weaker the acidity of the N−H proton is. Although the EDGs, on the contrary, can enhance the π-delocalization effect of the whole RAHB fragment, it contributes less to the hydrogen bonding.

2.5. Correlation analysis with Hammett empirical values

To provide insight into the correlation and contributions of different substituted hydrazones in terms of their configuration, the linear free energy relationship between hydrogen bond and Hammett substituent constants σ were examined.[41,42] We reasoned that if the E/Z equilibrium was determined by the IMHB, and the hydrogen bond interaction was highly influenced by the electronic effect of the substituent, a correlation between the E/Z equilibrium and substituent effect should be expected. The energies ΔG_R for the E/Z equilibrium for each compound was calculated based on their ^{1}H NMR spectra at equilibria, while their substituent effects were quantified by the Hammett empirical values. The hydrazones **4**−**15** were divided into two groups for study according to the substituent position, and a composite Hammett value σ_R ($\sigma_R = \sigma_p + \sigma_m$) was applied to plot.[43,44] As predicted, the Gibbs free energy changes $\Delta\Delta G_R$ ($\Delta\Delta G_R = \Delta G_R - \Delta G_H$, where ΔG_H indicates the Gibbs free energy of the unsubstituted reference hydrazone **1**) of both branches fit linear relationships with the composite Hammett values σ_R (Fig. 5, R^2 = 0.973 and 0.998), supporting our inference that the E/Z equilibria, IMHB strength and substituent effects are all correlated well with each other. In addition, a relatively larger slope was observed for substitution on the pyridine moiety than that for the phenyl ring. Upon comparing of alterations between compound **4** and **9** with that for **10** and **15**, the composite Hammett values were found to vary similarly ($\Delta\sigma_R$ = 2.21), but the energies for the E/Z equilibrium changed significantly, and were 1.73 times larger for substitution on pyridine ring than on the phenyl ring. This result indicates the substitution effect is more pronounced on the side of hydrogen bond acceptor than on donor.

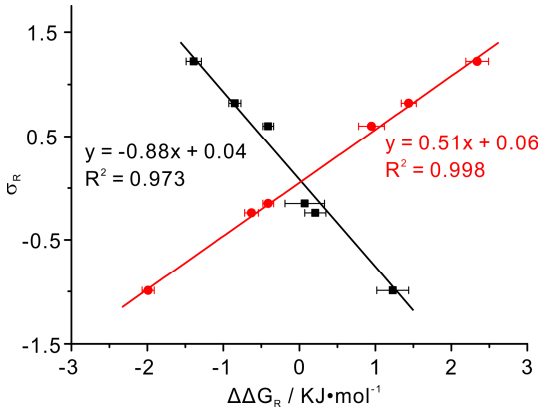

Fig. 5. Correlation of the energy change $\Delta\Delta G_R$ for substituted hydrazones **4**−**15** with the composite Hammett values σ_R. Black squares indicate the values for the substituents in the para position of the pyridine, red dots indicate the values for the substituent in the para position of the fluorobenzene ring.

3. Conclusions

The NMR experimental study of substituent effects on hydrogen bonding in a hydrazone-based switch revealed a linear correlation between the IMHB strengths and the E/Z isomerization capacity of these hydrazones. The anisotropy and push-pull effects of the substituents all contributed to the strength of IMHB, and further altered the isomerizations of hydrazones. This study can help us to better design molecular switches based on the manipulation of hydrogen bond.

4. Experimental section

4.1. General methods

All chemicals and solvents were purchased from commercial suppliers and were used without further purification unless otherwise specified. Column chromatography was carried out on Merck GEDURAN Si60 (40–63 μm). High-resolution electrospray ionization mass spectrometry (ESI-MS) was performed on a micro TOF II instrument.

NMR spectra were recorded on Bruker AVANCE 400 (400 MHz) spectrometers. The solvent signals were assigned by Fulmer et al.[45] All chemical shifts (δ) are quoted in ppm and coupling constants (J) are expressed in Hertz (Hz). The following abbreviations are used for convenience in reporting the multiplicity for NMR resonances: s = singlet, d = doublet, t = triplet, and m = multiplet. Data processing was performed with Topspin 2.0 software.

The calculation of Z/E ratio of the hydrazones by NMR: In NMR tubes, hydrazones were dissolved in the solvents, and ^{1}H NMR spectra were recorded with time until the Z/E isomerizations reached the equilibria. At equilibria, the ratios of Z/E isomers were not changed any more with time. Then their ratios can be calculated by integration of the proton signals from these two isomers.

Crystallographic data for compounds **1**−E, **1**−Z, **2**−E, **2**−Z, **3**−E and **3**−Z were collected at the the Analysis and Testing Center in Huazhong University of Science and Technology (HUST) on a Rigaku MM007 HF rotating anode (0.8 kW). Data were collected at the CuK wavelength. All data-collection strategies were based on Omega scans at 100(2) K. The X-ray source was equipped with high flux Osmic Varimax mirrors and a RAPID SPIDER semi-cylindrical image plate detector. The Rigaku Crystal Clear suite version 2.0 was used to index, integrate and scale the data with a multiscan absorption correction. Crystallographic data have been deposited with the CCDC, under deposition numbers CCDC 1882583-1882585 (**1**−E, **2**−E and **3**−E); 1891935−1891937 (**1**−Z, **2**−Z and **3**−Z).

The structures were solved by direct methods using SHELXT[46] and refined against F2 on all data by full-matrix least squares with SHELXL[47] following established refinement strategies.[48] The non−H atoms were refined with anisotropic temperature parameters. All hydrogen atoms were included into the model at geometrically calculated positions and refined using a riding model.

4.2. Preparation and Characterization

The E isomer of hydrazones **1**−**15** all can be easily to get by similar procedures. The corresponding aldehydes and hydrazine hydrochloride were added to the methanol solution, then the reaction mixture was heated under reflux for 10 hours. After the reaction was finished, removed the solvent in *vacuo*. The residue was dissolved in water and neutralized with saturated $NaHCO_3$ solution. Afterwards, extracted with dichloromethane and collected the organic layer. The organic layer were dried over by Na_2SO_4, filtered and concentrated. The residue was recrystallized by methanol to give the pure product.

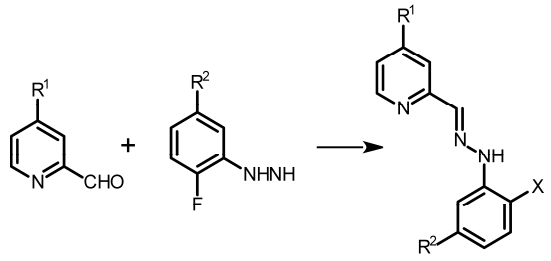

1-15 (E)

Compound **1**−E. ^{1}H NMR ($CDCl_3$, 400 MHz): δ 8.58 (d, J = 4.44 Hz, 1 H), 8.02−8.00 (m, 2 H), 7.88 (s, 1 H), 7.72−7.69 (m, 1 H) 7.64−7.60 (m, 1 H), 7.22−7.19 (q, J_1 = 6.38 Hz, J_2 = 5.10 Hz, 1 H), 7.14−7.10 (m, 1 H), 7.08−7.03 (q, J_1 = 10.72 Hz, J_2 = 8.28 Hz, 1 H), 6.86−6.81 (m, 1 H). ^{13}C NMR ($CDCl_3$, 100 MHz): δ 154.4, 151.1, 149.4, 148.7, 139.6, 136.4, 132.7, 132.6, 125.0, 125.0, 123.0, 120.3, 120.2, 120.0, 115.2, 115.0, 114.8, 114.8. ESI-HRMS: m/z calcd for $C_{12}H_{10}FN_3$ $[M+H]^+$ 216.0892 found 216.0917.

Compound **2**−E. ^{1}H NMR ($CDCl_3$, 400 MHz): δ 8.58 (d, J = 4.56 Hz, 1 H), 8.30 (s, 1 H), 8.02 (d, J = 7.96 Hz, 1 H), 7.92 (s, 1 H), 7.72−7.69 (m, 1 H), 7.65 (d, J = 8.16 Hz, 1 H), 7.31 (d, J = 7.96 Hz, 1 H), 7.22−7.19 (m, 1 H), 6.86−6.82 (m, 1 H). ^{13}C NMR ($CDCl_3$, 100 MHz): δ 154.3, 149.5, 140.2, 140.0, 136.4, 129.4, 128.1, 123.1, 120.8, 120.0, 117.5, 114.5. ESI-HRMS: m/z calcd for $C_{12}H_{10}ClN_3$ $[M+H]^+$ 233.0534 found 233.0591.

Compound **3**−E. ^{1}H NMR ($CDCl_3$, 400 MHz): δ 8.58 (d, J = 4.32 Hz, 1 H), 8.31 (s, 1 H), 8.02 (d, J_1 = 8.04 Hz, 1 H), 7.92 (s, 1 H), 7.73−7.71 (m, 1 H), 7.64−7.62 (m, 1 H), 7.47−7.45 (dd, J_1 = 7.92 Hz, J_2 = 1.04 Hz, 1 H), 7.31−7.27 (m, 1 H), 7.22−7.19 (m, 1 H), 6.80−6.76 (m, 1 H). ^{13}C NMR ($CDCl_3$, 100 MHz): δ 154.3, 149.5, 141.1, 140.0, 136.4, 132.5, 128.7, 123.1, 121.4, 120.0, 114.9, 107.3. ESI-HRMS: m/z calcd for $C_{12}H_{10}BrN_3$ $[M+H]^+$ 277.0038 found 277.0051.

Compound **4**−E. ^{1}H NMR ($CDCl_3$, 400 MHz): δ 8.71 (d, J = 4.96 Hz, 1 H), 8.23 (s, 1 H), 7.86 (s, 1 H), 7.65−7.61 (t, J = 8.00 Hz, 1 H), 7.38 (d, J = 3.92 Hz, 1 H),7.18−7.15 (t, J = 7.69 Hz, 1 H), 7.10−7.05 (q, J_1 = 11.14 Hz, J_2 = 8.38 Hz, 1 H), 6.92−6.88 (m, 1 H). ^{13}C NMR ($CDCl_3$, 100 MHz): δ 155.9, 150.3, 137.1, 131.9, 131.8, 125.2, 125.2, 123.4, 121.8, 121.2, 121.2, 120.9, 116.8, 115.4, 115.2, 114.9. ESI-HRMS: m/z calcd for $C_{13}H_9FN_4$ $[M+H]^+$ 241.0845 found 241.0892.

Compound **5**−E. ^{1}H NMR ($CDCl^3$, 400 MHz): δ 8.70 (d, J = 5.00 Hz, 1 H), 8.51 (s, 1 H), 8.13 (s, 1 H), 7.93 (s, 1 H), 7.74 (d, J = 4.80 Hz, 1 H), 7.70−7.66 (t, J = 8.16 Hz, 1 H), 7.17−7.13 (t, J = 7.78 Hz, 1 H), 7.09−7.04 (m, 1 H), 6.89−6.84 (q, J = 6.69 Hz, m, 1 H), 4.00 (s, 3 H). ^{13}C NMR ($CDCl_3$, 100 MHz): δ 165.8, 155.5, 151.2, 150.2, 148.8, 138.6, 137.9, 132.4, 125.1, 121.8, 120.7, 119.4, 115.2, 115.1, 115.0, 52.9. ESI-HRMS: m/z calcd for $C_{13}H_9FN_4$ $[M+H]^+$ 274.0947 found 274.1016.

Compound **6**−E. ^{1}H NMR ($CDCl_3$, 400 MHz): δ 8.46 (d, J = 5.32 Hz, 1 H), 8.11 (s, 1 H), 8.00 (d, J = 1.52 Hz, 1 H), 7.83 (s, 1 H), 7.65−7.61 (t, J = 7.86 Hz, 1 H), 7.20−7.19 (dd, J_1 = 5.30 Hz, J2 = 1.86 Hz, 1 H), 7.16−7.12 (t, J = 7.74 Hz, 1 H), 7.09−7.04 (q, J_1 = 10.74 Hz, J_2 = 8.34 Hz, 1 H), 6.89−6.84 (m, 1 H). ^{13}C NMR ($CDCl_3$, 100 MHz): δ 155.9, 151.2, 150.2, 148.8, 144.6, 138.0, 132.3, 125.1, 125.1, 123.1, 120.8, 119.9, 115.3, 115.1, 114.9. ESI-HRMS: m/z calcd for $C_{12}H_9ClFN_3$ $[M+H]^+$ 251.0440 found 251.0503.

Compound **7**−E. ^{1}H NMR ($CDCl_3$, 400 MHz): δ 8.43 (d, J = 5.00 Hz, 1 H), 7.99 (s, 1 H), 7.86 (s, 1 H), 7.82 (s, 1 H), 7.66−7.62 (t, J = 7.74 Hz, 1 H), 7.14−7.11 (t, J = 7.68 Hz, 1 H), 7.07-7.02 (m, 2 H), 6.86−6.81 (m, 1 H). ^{13}C NMR ($CDCl_3$, 100 MHz): δ 154.1, 151.1, 149.2, 148.7, 147.5, 139.8, 132.7, 125.0, 125.0, 124.2, 120.6, 120.2, 120.1, 115.2, 115.0, 114.8, 114.8, 21.3. ESI-HRMS: m/z calcd for $C_{13}H_{12}FN_3$ $[M+H]^+$ 230.1049 found 230.1076.

Compound **8**−E. ^{1}H NMR ($CDCl_3$, 400 MHz): δ 8.39 (d, J = 5.72 Hz, 1 H), 8.00 (s, 1 H), 7.85 (s, 1 H), 7.63-7.59 (t, J = 7.78 Hz, 1 H), 7.51 (d, J = 2.36 Hz, 1 H), 7.14−7.10 (t, J = 7.74 Hz, 1 H), 7.08−7.03 (q, J_1 = 10.70 Hz, J_2 = 8.30 Hz, 1 H), 6.86−6.81 (m, 1 H), 6.77−6.75 (dd, J_1 = 5.72 Hz, J_2 = 2.48 Hz, 1 H), 3.93 (s, 3 H). ^{13}C NMR ($CDCl_3$, 100 MHz): δ 166.1, 156.0, 151.1, 150.5, 148.7, 139.6, 132.6, 125.0, 125.0, 120.3, 120.2, 115.2, 115.0, 114.8, 114.8, 110.4, 104.6, 55.4. ESI-HRMS: m/z calcd for $C_{13}H_{12}FN_3O$ $[M+H]^+$ 246.0998 found 246.1112.

Compound **9**−E. ^{1}H NMR ($CDCl_3$, 400 MHz): δ 8.22 (d, J = 6.00 Hz, 1 H), 7.95 (s, 1 H), 7.83 (s, 1 H), 7.63−7.59 (t, J = 8.06 Hz, 1 H), 7.20 (d, J = 1.60 Hz, 1 H), 7.13−7.09 (t, J = 7.66 Hz, 1 H), 7.07−7.02 (q, J = 6.61 Hz, 1 H), 6.84−6.79 (q, J = 6.66 Hz, 1 H), 6.48−6.47(m, 1 H), 3.08 (s, 6 H). ^{13}C NMR ($CDCl_3$, 100 MHz): δ 154.7, 153.9, 151.1, 149.3, 148.7, 140.7, 132.9, 124.9, 119.9, 115.1, 115.0, 114.7, 106.8, 102.0, 39.4. ESI-HRMS: m/z calcd for $C_{13}H_{12}FN_3O$ $[M+H]^+$ 259.1314 found 246.1963.

Compound **10**−E. ^{1}H NMR ($CDCl_3$, 400 MHz): δ 8.60 (d, J = 4.40 Hz, 1 H), 8.05−8.02 (m, 2 H), 7.93−7.90 (m, 2 H), 7.78−7.74 (t, J = 7.62 Hz, 1 H), 716−7.11 (m, 2 H). ^{13}C NMR ($CDCl_3$, 100 MHz): δ 153.6, 149.6, 141.9, 136.7, 124.4, 123.7, 120.3, 118.7, 118.4, 116.3, 116.2, 109.4. ESI-HRMS: m/z calcd for $C_{14}H_{12}FN_3O_2$ $[M+H]^+$ 241.0845 found 241.0864.

Compound **11**−E. ^{1}H NMR ($CDCl_3$, 400 MHz): δ 8.59 (d, J = 4.56 Hz, 1 H), 8.28 (d, J = 7.56 Hz, 1 H), 8.10 (d, J = 7.92 Hz, 1 H), 8.03 (s, 1 H), 7.76−7.72 (t, J = 7.44 Hz, 1 H), 7.58−7.55 (m, 1 H), 7.25−7.22 (m, 1 H), 7.13−7.08 (q, J_1 = 10.86 Hz, J_2 = 8.62 Hz, 1 H), 3.94 (s, 3 H). ^{13}C NMR ($CDCl_3$, 100 MHz): δ 166.7, 154.0, 151.3, 149.4, 140.7, 136.5, 132.8, 132.7, 127.4, 127.4, 123.3, 122.2, 120.3, 116.2, 116.2, 115.3, 115.1, 52.4. ESI-HRMS: m/z calcd for $C_{14}H_{12}FN_3O_2$ $[M+H]^+$ 274.0947 found 274.0995.

Compound **12**−E. ^{1}H NMR ($CDCl_3$, 400 MHz): δ 8.59 (d, J = 4.44 Hz, 1 H), 8.04 (d, J = 8.00 Hz, 1 H), 7.98 (s, 1 H), 7.89 (s, 1 H), 7.75−7.71 (t, J = 7.10 Hz, 1 H), 7.61−7.58 (dd, J_1 = 7.10 Hz, J_2 = 2.42 Hz, 1 H), 7.25−7.22 (m, 1 H), 7.00−6.95 (q, J_1 = 11.06 Hz, J_2 = 8.70 Hz, 1 H), 6.80−6.76 (m, 1 H). ^{13}C NMR ($CDCl_3$, 100 MHz): δ 153.9, 149.5, 140.8, 136.5, 133.6, 133.5, 130.4, 123.4, 120.2, 119.7, 119.6, 116.2, 116.0, 114.7. ESI-HRMS: m/z calcd for $C_{12}H_9ClFN_3$ $[M+H]^+$ 251.0440 found 251.0610.

Compound **13**−E. ^{1}H NMR ($CDCl^3$, 400 MHz): δ 8.58 (d, J = 4.52 Hz, 1 H), 8.02 (d, J = 8.00 Hz, 1 H), 7.98 (s, 1 H), 7.86 (s, 1 H), 7.73−7.69 (m, 1 H), 7.43 (d, J = 6.84 Hz, 1 H), 7.26−7.19 (q, J_1 = 6.38 Hz, J_2 = 5.14 Hz, 1 H), 6.95−6.90 (q, J_1 = 11.48 Hz, J_2 = 8.32 Hz, 1 H), 6.64−6.61 (m, 1 H), 2.35 (s, 3 H). ^{13}C NMR ($CDCl_3$, 100 MHz): δ 154.4, 149.4, 147.1, 139.3, 136.4, 134.7, 134.7, 132.1, 132.0, 122.9, 120.7, 120.7, 115.1, 115.1, 114.8, 114.6, 21.3. ESI-HRMS: m/z calcd for $C_{13}H_{12}FN_3$ $[M+H]^+$ 230.1049 found 230.1104.

Compound **14**−E. ^{1}H NMR ($CDCl_3$, 400 MHz): δ 8.57 (d, J = 4.40 Hz, 1 H), 8.02−8.00 (d, 2 H), 7.87 (s, 1 H), 7.72−7.69 (t, J = 7.20 Hz, 1 H), 7.22−7.16 (m, 2 H), 6.98-6.93 (q, J_1 = 10.96 Hz, J_2 = 9.00 Hz, 1 H), 6.36−6.32 (m, 1 H), 3.83 (s, 3 H). ^{13}C NMR ($CDCl_3$, 100 MHz): δ 166.7, 154.0, 153.8, 151.3, 149.4, 140.7, 136.5, 132.8, 132.7, 127.4, 127.4, 123.3, 122.2, 122.1, 120.3, 116.3, 116.2, 115.3, 115.1, 52.4. ESI-HRMS: m/z calcd for $C_{13}H_{12}FN_3O$ $[M+H]^+$ 246.0998 found 246.1085.

Compound **15**−E. ^{1}H NMR ($CDCl_3$, 400 MHz): δ 8.57 (d, J = 4.12 Hz, 1 H), 8.00 (d, 2 H), 7.86 (s, 1 H), 7.72−7.68 (t, J = 7.12 Hz, 1 H), 7.21−7.18 (m, 1 H), 7.01−6.98 (dd, J_1 = 6.98 Hz, J_2 = 3.02 Hz, 1 H), 6.95−6.90 (q, J_1 = 11.80 Hz, J_2 = 9.08 Hz, 1 H), 6.21−6.17 (m, 1 H), 2.96 (s, 6 H). ^{13}C NMR ($CDCl_3$, 100 MHz): δ 154.5, 149.3, 148.5, 144.4, 142.2, 139.0, 136.4, 132.5, 132.4, 122.9, 119.9, 115.3, 115.1, 104.6, 104.6, 99.2, 41.5. ESI-HRMS: m/z calcd for $C_{14}H_{15}FN_4$ $[M+H]^+$ 259.1314 found 259.1376.

The corresponding aldehydes for synthesis of hydrazones **1**−**15** can be obtained by reduction of the commercial esters except for 4-(dimethylamino)picolinaldehyde **18**. The corresponding hydrazines can be synthesized easily from the commercial amines except for compound methyl 4-fluoro-3-hydrazinylbenzoate **22** and 4-fluoro-3-hydrazinyl-*N*,*N*-dimethylaniline **27**. The synthetic procedures of **18**, **22** and **27** are

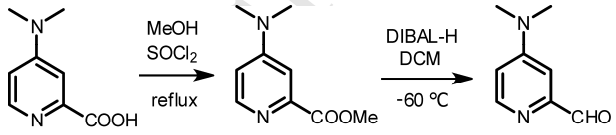

in the following.

Compound **16**.[49] A solution of 4-chloropicolinic acid (0.78 g, 5 mmol) in aqueous dimethylamine (40 %, 10 ml) was stirred at 100 °C for 5 h in a sealed tube. The resulting solution was concentrated in *vacuo*, then dissolved in EtOAc (50 ml) and washed with saturated aqueous $NaHCO_3$ (50 ml) twice. The organic phase was dried over $MgSO_4$ and evaporated in *vacuo* to afford compound **16** (0.79 g, 95 %). ^{1}H NMR (DMSO-d_6, 400 MHz): δ 8.20 (d, J = 7.48 Hz, 1 H), 7.43 (d, J = 2.98 Hz, 1 H), 7.10 (dd, J_1 = 3.01 Hz, J_2 = 7.53 Hz, 1 H), 3.27 (s, 6 H). ESI-HRMS: m/z calcd for $C_8H_{10}N_2O_2$ $[M+H]^+$ 189.0634 found 189.0638.

Compound **17**. Thionyl chloride (5 ml) was slowly added to a solution of compound **16** (0.83 g, 5 mmol) in MeOH (30 ml). The solution was then heated to reflux for 12 h and concentrated in *vacuo*. The residue was dissolved in dichloromethane (DCM) and washed with saturated aqueous NaCl, dried over $MgSO_4$ and evaporated in *vacuo* to afford compound **17** (0.80 g, 89 %). ^{1}H NMR ($CDCl_3$, 400 MHz): δ 8.32 (d, J = 5.76, 1 H), 7.40 (s, 1 H), 6.60 (d, J = 3.24 Hz, 1 H), 3.98 (s, 3 H), 3.06 (s, 6 H). ESI-HRMS: m/z calcd for $C_9H_{12}N_2O_2$ $[M+H]^+$ 181.0932 found 181.0987.

Compound **18**.[50] Compound **17** (0.90 g, 5 mmol) was dissolved in anhydrous DCM (25 ml) and the solution was cooled to −60 °C. Diisobutyl aluminum hydride (DIBAL−H) (1.5 M in toluene, 6.67 ml) was dropwised. After 5 minutes at the end of addition, the reaction mixture was treated with the addition of MeOH (5 ml) and then with aqueous solution of NaOH (10 %, 20 ml). The organic layers were dried over $MgSO_4$, filtered and concentrated to give the product **18** (0.57 g, 76 %). ^{1}H NMR ($CDCl_3$, 400 MHz): δ 9.99 (s, 1 H), 8.38 (d, J = 5.80, 1 H), 7.18 (d, J = 2.20, 1 H, 6.66−6.64 (q, J = 2.66 Hz, 1 H), 3.07(s, 6 H). ESI-HRMS: m/z calcd for $C_8H_{10}N_2O$ $[M+H]^+$ 151.0827 found 151.0886.

Compound **19**.[51] To a solution of 4-fluorobenzoic acid (2.80 g, 20 mmol) in concentrated H_2SO_4 (25 ml) in an ice bath was added potassium nitrate (2.20 g, 22 mmol) in portions within 30 minutes. The ice bath was removed and the mixture was stirred at ambient temperature overnight. To the mixture was added

crushed ice at room temperature, the residue was filtered to give the product **19** (2.41 g, 65 %). ^{1}H NMR (DMSO-d_6, 400 MHz): δ 13.69 (br, 1 H), 8.57 (d, J = 5.64, 1 H), 8.32−8.30 (m, 1 H), 7.75−7.70 (m, 1 H). ESI-HRMS: m/z calcd for $C_8H_{10}N_2O$

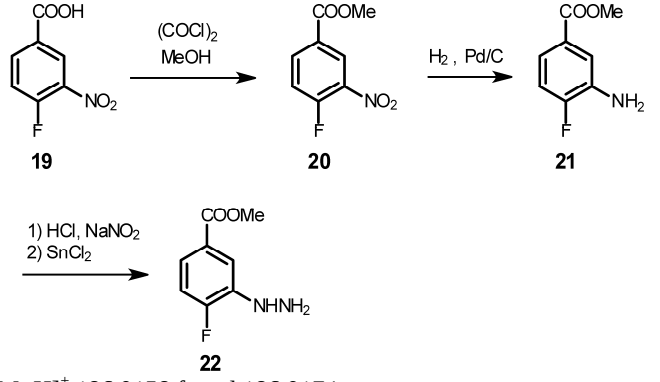

$[M+H]^+$ 186.0158 found 186.0174.

Compound **20**. To a solution of compound **19** (1.85 g, 10 mmol) in anhydrous DCM (30 ml) was added $(COCl)_2$ (1.70 ml, 20 mmol), then the mixture was stirred 3 h at room temperature. The resulting solution was concentrated in *vacuo*, then dissolved in anhydrous DCM (20 ml) and MeOH (20 ml) and stirred for 2 h. The resulting solution was concentrated in *vacuo* again, and dissolved in DCM and washed with saturated aqueous NaCl. The organic phase was dried over $MgSO_4$ and evaporated in *vacuo* to afford compound 20 (1.83 g, 92 %). ^{1}H NMR ($CDCl_3$, 400 MHz): δ 8.76−8.74 (dd, J_1 = 1.70, J_2 = 7.06, 1 H), 8.34−8.31 (m, 1 H), 7.41−7.36 (t, J = 9.46 Hz, 1 H), 3.98 (s, 3 H). ESI-HRMS: m/z calcd for $C_8H_6FNO_4$ $[M+H]^+$ 200.0314 found 200.0405.

Compound **21**. Compound **20** (1.00 g, 5 mmol) underwent hydrogenation in the solution of EtOAc (10 ml) and MeOH (10 ml) at H_2 atmosphere for 5 h using Pd/C (0.10 g, 10 %) as the catalyst. The reaction was then filtered and the solvent was removed in *vacuo* to afford the compound **21** (0.81 g, 96 %). ^{1}H NMR ($CDCl_3$, 400 MHz): δ 7.49−7.47 (dd, J_1 = 1.76, J_2 = 8.60, 1 H), 7.43−7.39 (m, 1 H), 7.04−6.99 (q, J_1 = 8.62, J_2 = 10.46, 1 H), 3.88 (s, 3 H), 3.82 (br, 2 H). ESI-HRMS: m/z calcd for $C_8H_8FNO_2$ $[M+H]^+$ 170.0573 found 170.0618.

Compound **22**.[52] To a suspension of compound **21** (1.01 g, 6 mmol) in hydrochloric acid (13 ml, 37 %) at 0 °C was added a cold solution of sodium nitrite (0.50 g, 7.2 mmol) in water (5 ml) maintaining the temperature below 5 °C. The resultant solution was stirred in an ice bath for 30 min before the addition of a solution of tin (II) chloride dehydrate (4.06 g, 18 mmol) in hydrochloric acid (5 ml, 37 %) maintaining the temperature below 5 °C. The resultant suspension was stirred at 0 °C for 3 h and the suspension filtered and then dissolved in DCM, washed with saturated $NaHCO_3$, dried over by $MgSO_4$ to get the compound **22** (1.01 g, 92 %). ^{1}H NMR ($CDCl_3$, 400 MHz): δ 7.79−7.77 (m, 1 H), 7.46 (s, 1 H), 7.04−6.99 (m, 1 H), 5.48 (br, 1 H), 3.91 (s, 3 H) 3.62 (br, 2 H). ESI-HRMS: m/z calcd for $C_8H_9FN_2O_2$ $[M+H]^+$ 185.0682 found 185.0664.

Compound **23**. To a solution of compound **19** (1.03 g, 5.6 mmol) in anhydrous DCM (15 ml) was added $(COCl)_2$ (1.7 ml, 20 mmol), the mixture was stirred for 5 h at room temperature, and then dried in *vacuo*. The residue was dissolved in anhydrous DCM (20 ml), and trimethylsilyl azid ($TMSN_3$) (2.21 ml, 16.8 mmol) was added to the solution and the reaction was stirred overnight. The solvent was removed in *vacuo*, and dried for 2 h. The residue was redissolved in anhydrous toluene (20 ml) and 2-trimethylsilyl ethanol (1.61 ml, 12.6 mmol) was added, the mixture was stirred for 10 h at 90 °C. The resulting solution was concentrated in *vacuo*, and then dissolved in DCM. The solution washed with saturated aqueous NaCl and the organic layer died over by $MgSO_4$, and evaporated in *vacuo* to give the product **23** (1.26 g, 75 %). ^{1}H NMR (DMSO-d_6, 400 MHz): δ 10.06 (s, 1 H), 8.34 (d, J = 4.40 Hz, 1 H), 7.77−7.75 (m, 1 H), 7.56−7.51 (t, J = 10.10 Hz, 1 H), 4.23−4.19 (t, J = 8.44 Hz, 2 H), 1.04−1.00 (t, J = 8.46 Hz, 1 H), 0.05 (s, 9 H). ESI-HRMS: m/z calcd for $C_{12}H_{17}FN_2O_4Si$ $[M+H]^+$ 301.0975 found 301.0822.

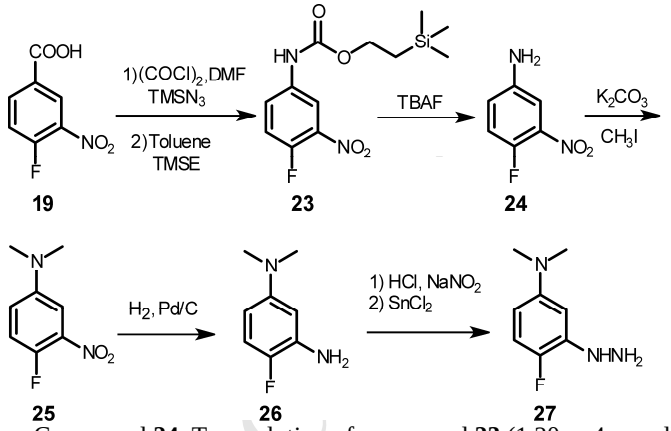

Compound **24**. To a solution of compound **23** (1.20 g, 4 mmol) in THF (20 ml) was added tetrabutylammonium fluoride (3.13 g, 12 mmol) and the reaction mixture was stirred at room temperature for 10 h. The solvent was removed in *vacuo*, the residue was dissolved in DCM, and dried over by $MgSO_4$, then concentrated in *vacuo* to get the compound **24** (0.59 g, 95 %). ^{1}H NMR (DMSO-d_6, 400 MHz): δ 7.24−7.19 (m, 2 H), 6.92−6.88 (m, 1 H), 5.63 (s, 2 H). ESI-HRMS: m/z calcd for $C_6H_5FN_2O_2$ $[M+H]^+$ 157.0369 found 157.0375.

Compound **25**. To a solution of compound **24** (0.31 g, 2 mmol) and K_2CO_3 (1.38 g, 10 mmol) in anhydrous *N*,*N*-dimethylformamide (DMF) (5 ml) was added CH_3I (0.35 g, 2.5 mmol), and the reaction mixture was stirred for 10 h at 80 °C. After cooling down the reaction to room temperature was added DCM (50 ml) to the solution, and washed with saturated $NaHCO_3$. The organic layer dried over by $MgSO_4$ and concentrated in *vacuo* to give the product **25** (0.34 g, 92 %). ^{1}H NMR (DMSO-d_6, 400 MHz): δ 7.41−7.36 (m, 1 H), 7.23−7.21 (m, 1 H), 7.12−7.09 (m, 1 H), 2.95 (s, 6 H). ESI-HRMS: m/z calcd for $C_8H_9FN_2O_2$ $[M+H]^+$ 185.0682 found 185.0749.

Compound **26**. The similar procedure as described in synthesizing compound **21**. ^{1}H NMR ($CDCl_3$, 400 MHz): δ 6.88-6.83 (t, J = 9.76 Hz, 1 H), 8.34 (dd, J_1 = 2.68 Hz, J_1 = 7.56 Hz, 1 H), 6.10−6.06 (m, 1 H), 3.65 (s, 2 H), 2.86 (s, 6 H). ESI-HRMS: m/z calcd for $C_8H_{11}FN_2$ $[M+H]^+$ 155.0940 found 155.1032.

Compound **27**. The similar procedure as described in synthesizing compound **22**. ^{1}H NMR (DMSO-d6, 400 MHz): δ 10.28 (s, 3 H), 8.35 (br, 1 H), 7.19−7.14 (m, 1 H), 7.03 (s, 1 H), 6.69 (s, 1 H), 2.96 (s, 6 H).

Acknowledgments

This work was supported by the National Natural Science Foundation of China (no. 21602069, 21871101); and the Natural Science Foundation of Hubei Scientific Committee (no. 2017CFA036). We are grateful to the Analysis and Testing Center in Huazhong University of Science and Technology for their help with material characterizations.

Appendix A. Supplementary data

Supplementary data to this article can be found online at

References and notes

1. Desiraju, G. R.; Steiner, T. *The Weak Hydrogen Bond: In Structural Chemistry and Biology*; Oxford University Press, **1999**.
2. Steiner, T. *Angew. Chem. Int. Ed.* **2002,** *41*, 48−76.
3. Desiraju, G. R. *Angew. Chem. Int. Ed.* **2011,** *50*, 52−59.
4. Jeffrey, G. A.; Jeffrey, G. A. *An introduction to hydrogen bonding*; Oxford university press New York, **1997**; Vol. 32.
5. Scheiner, S. *Hydrogen bonding: a theoretical perspective*; Oxford University Press on Demand, **1997**.
6. Grabowski, S. J. *Hydrogen bonding: new insights*; Springer, **2006**; Vol. 3
7. Kortemme, T.; Morozov, A. V.; Baker, D. *J. Mol. Biol.* **2003,** *326*, 1239−1259.
8. Biedermann, F.; Schneider, H.-J. r. *Chem. Rev.* **2016,** *116*, 5216−5300.
9. Prins, L. J.; Reinhoudt, D. N.; Timmerman, P. *Angew. Chem. Int. Ed.* **2001,** *40*, 2382−2426
10. Zhang, D.-W.; Zhao, X.; Li, Z.-T. *Acc. Chem. Res.* **2014,** *47*, 1961−1970.
11. Ren, C.; Xu, S.; Xu, J.; Chen, H.; Zeng, H. *Org. lett.* **2011,** *13*, 3840−3843.
12. Saraogi, I.; Hamilton, A. D. *Chem. Soc. Rev.* **2009,** *38*, 1726−1743.
13. Li, X.; Wu, Y.-D.; Yang, D. *Acc. Chem. Res.* **2008,** *41*, 1428−1438.
14. Adhikary, R.; Zimmermann, J. r.; Liu, J.; Forrest, R. P.; Janicki, T. D.; Dawson, P. E.; Corcelli, S. A.; Romesberg, F. E. *J. Am. Chem. Soc.* **2014,** *136*, 13474−13477.
15. Zhang, D.-W.; Zhao, X.; Hou, J.-L.; Li, Z.-T. *Chem. Rev.* **2012,** *112*, 5271−5316.
16. Li, C.; Ren, S. F.; Hou, J. L.; Yi, H. P.; Zhu, S. Z.; Jiang, X. K.; Li, Z. T. *Angew. Chem. Int. Ed.* **2005,** *44*, 5725−5729.
17. Eisenberg, D. Proc. Natl. Acad. Sci. **2003,** *100*, 11207−11210.
18. Chaur, M. N.; Collado, D.; Lehn, J. M. *Chem–Eur. J.* **2011,** *17*, 248−258.
19. Aprahamian, I. *Chem. Commun.* **2017,** *53*, 6674−6684.
20. Lu, C.; Htan, B.; Ma, C.; Liao, R. Z.; Gan, Q. *Eur. J. Org. Chem.* **2018,** *2018*, 7046−7050.
21. van Dijken, D. J.; Kovaříček, P.; Ihrig, S. P.; Hecht, S. *J. Am. Chem. Soc.* **2015,** *137*, 14982−14991.
22. Su, X.; Aprahamian, I. *Chem. Soc. Rev.* **2014,** *43*, 1963−1981.
23. Gholipour, A.; Neyband, R. S.; Farhadi, S. *Chem. Phys. Lett.* **2017,** *676*, 6−11.
24. Hansch, C.; Leo, A.; Taft, R. *Chem. Rev.* **1991,** *91*, 165−195.
25. Qian, H.; Pramanik, S.; Aprahamian, I. *J. Am. Chem. Soc.* **2017,** *139*, 9140−9143.
26. Favaro, D. C.; Contreras, R. n. H.; Tormena, C. F. *J. Phys. Chem. A* **2013,** *117*, 7939−7945.
27. Brunner, E.; Sternberg, U. Prog. Nucl. Mag. Res. Sp. **1998,** *32*, 21−57.
28. Shenderovich, I. G.; Tolstoy, P. M.; Golubev, N. S.; Smirnov, S. N.; Denisov, G. S.; Limbach, H.-H. *J. Am. Chem. Soc.* **2003,** *125*, 11710−11720.
29. Zhu, Y.-Y.; Yi, H.-P.; Li, C.; Jiang, X.-K.; Li, Z.-T. *Cryst. Growth Des.* **2008,** *8*, 1294−1300.
30. Lu, B.-Y.; Li, Z.-M.; Zhu, Y.-Y.; Zhao, X.; Li, Z.-T. *Tetrahedron* **2012,** *68*, 8857-8862.
31. Šimůnek, P.; Bertolasi, V.; Lyčka, A.; Macháček, V. *Org. Biomol. Chem.* **2003,** *1*, 3250−3256.
32. Šimůnek, P.; Svobodová, M.; Bertolasi, V.; Pretto, L.; Lyčka, A.; Macháček, V. *New J. Chem.* **2007,** *31*, 429−438.
33. Gilli, G.; Bellucci, F.; Ferretti, V.; Bertolasi, V. *J. Am. Chem. Soc.* **1989,** *111*, 1023−1028.
34. Gilli, P.; Bertolasi, V.; Pretto, L.; Ferretti, V.; Gilli, G. *J. Am. Chem. Soc.* **2004,** *126*, 3845−3855.
35. Lee, H. Y.; Song, X.; Park, H.; Baik, M.-H.; Lee, D. *J. Am. Chem. Soc.* **2010,** *132*, 12133−12144.
36. Gilli, P.; Bertolasi, V.; Pretto, L.; Lyčka, A.; Gilli, G. *J. Am. Chem. Soc.* **2002,** *124*, 13554−13567.
37. Steiner, T. *Chem. Commun.* **1998**, 411−412.
38. Sobczyk, L.; Grabowski, S. J.; Krygowski, T. M. *Chem. Rev.* **2005,** *105*, 3513−3560.
39. Gilli, P.; Pretto, L.; Bertolasi, V.; Gilli, G. *Acc. Chem. Res.* **2008,** *42*, 33−44.
40. Bertolasi, V.; Nanni, L.; Gilli, P.; Ferretti, V.; Gilli, G.; Issa, Y.; Sherif, O. *New J. Chem.* **1994,** *18*, 251−261.
41. Chapman, N. *Correlation analysis in chemistry: Recent advances*; Springer Science & Business Media, 2012.
42. Bertolasi, V.; Gilli, P.; Ferretti, V.; Gilli, G. *J. Chem. Soc.* **1997**, *2*, 945−952.
43. Zhu, W.; Tan, X.; Shen, J.; Luo, X.; Cheng, F.; Mok, P. C.; Ji, R.; Chen, K.; Jiang, H. *J. Phys. Chem. A* **2003,** *107*, 2296−2303.
44. Ebrahimi, A.; Habibi, M.; Neyband, R. S.; Gholipour, A. R. *Phys. Chem. Chem. Phys.* **2009,** *11*, 11424−11431.
45. Fulmer, G. R.; Miller, A. J.; Sherden, N. H.; Gottlieb, H. E.; Nudelman, A.; Stoltz, B. M.; Bercaw, J. E.; Goldberg, K. I. *Organometallics* **2010,** *29*, 2176−2179.
46. Sheldrick, G. M. Acta Crystallogr., Sect. A: Found. Adv **2014,** *70*, C1437.
47. Sheldrick, G. M. Acta Crystallogr., Section C: Structural Chemistry **2015,** *71*, 3−8.
48. Müller, P. *Cryst. Res.* **2009,** *15*, 57−83.
49. Yeoh, K. K.; Chan, M. C.; Thalhammer, A.; Demetriades, M.; Chowdhury, R.; Tian, Y.-M.; Stolze, I.; McNeill, L. A.; Lee, M. K.; Woon, E. C. *Org. Biomol. Chem.* **2013,** *11*, 732−745.
50. Le Provost, R.; Wille, T.; Louise, L.; Masurier, N.; Müller, S.; Reiter, G.; Renard, P.-Y.; Lafont, O.; Worek, F.; Estour, F. *Org. Biomol. Chem.* **2011,** *9*, 3026−3032.
51. Shang, J.; Gallagher, N. M.; Bie, F.; Li, Q.; Che, Y.; Wang, Y.; Jiang, H. *J. Org. Chem.* **2014,** *79*, 5134−5144.
52. Green, N. J.; Xiang, J.; Chen, J.; Chen, L.; Davies, A. M.; Erbe, D.; Tam, S.; Tobin, J. F. *Bioorg. Med. Chem.* **2003,** *11*, 2991−3013